

Copy 206
RM A54E06

NACA RM A54E06

TECH LIBRARY KAFB, NM



RESEARCH MEMORANDUM

6434
INVESTIGATION OF A FLOW DEFLECTOR AND AN AUXILIARY
SCOOP FOR IMPROVING OFF-DESIGN PERFORMANCE
OF NOSE INLETS

By Warren E. Anderson and Richard Scherrer

Ames Aeronautical Laboratory
Moffett Field, Calif.

Classification cancelled (or changed to Unclassified)

By Authority of Nasa Tech Rd. Admin. #27
(OFFICER AUTHORIZED TO CHANGE)

By S. James S. Jr.
NAME AND

NK

.....
GRADE OF OFFICER MAKING CHANGE)

24 Mar. 61
DATE

**NATIONAL ADVISORY COMMITTEE
FOR AERONAUTICS**

WASHINGTON

July 20, 1954



0143349

S
NACA RM A54E06

NATIONAL ADVISORY COMMITTEE FOR AERONAUTICS

RESEARCH MEMORANDUMINVESTIGATION OF A FLOW DEFLECTOR AND AN AUXILIARY
SCOOP FOR IMPROVING OFF-DESIGN PERFORMANCE
OF NOSE INLETS

By Warren E. Anderson and Richard Scherrer

SUMMARY

Flow deflectors which extended forward of an open-nose inlet for improving positive angle-of-attack performance and auxiliary scoops for use at off-design engine air-flow conditions were investigated at low angles of attack to determine their effect on net inlet performance. Tests were conducted on two flow deflectors and two auxiliary scoops in the Ames 6- by 6-foot supersonic wind tunnel. The Mach number range of these tests was from 0 to 1.50.

The results show that a deflector inlet and a basic open-nose inlet have about the same net performance at low angles of attack although the flow steadiness characteristics of the deflector inlet are the less desirable. Thus, a flow deflector which improves performance at angles of attack causes no significant loss in performance at the conditions for high-speed flight.

With an auxiliary scoop, the maximum mass-flow ratio of the nose inlet was increased in proportion to the area increase represented by the auxiliary scoop; however, pressure recovery was slightly reduced and drag was increased. The net performance based on effective thrust ratios indicated that a variable auxiliary-scoop inlet can be advantageous for certain flight applications in which the engine-inlet matching problem is critical.

INTRODUCTION

Open-nose air-induction systems are known to give satisfactory performance at Mach numbers up to about 1.50 since the pressure loss through a normal shock wave is relatively small in this Mach number range. The maximum performance of this type of fixed system is considerably reduced, however, by two adverse characteristics. First, the

pressure recovery decreases at moderately high angles of attack as a result of the sharp lip profiles which are required by drag considerations for supersonic aircraft, and, second, a substantial loss in net thrust can be experienced at off-design engine-inlet operating conditions when the air flow required by the engine varies considerably from the air flow for which the inlet area was designed. Recent research has been directed toward the improvement of these characteristics. References 1 to 4 have established that good pressure recovery can be maintained at positive angles of attack when the inlet incorporates a deflecting surface such as a conical body or flat plate. Variable air-induction systems have been frequently proposed as a means to improve off-design engine-inlet operation. The bypass and translating spike systems which are compared in reference 5 show that considerable improvement in off-design operation is possible. Also, an auxiliary-scoop system was reported in references 6 and 7 which shows promise in this regard. Such a system is particularly attractive for aircraft with critical requirements at widely different air-flow conditions, such as take-off and maximum speed, and for aircraft required to have high maximum speeds at low altitudes. If this latter requirement is fulfilled, the take-off problem becomes more severe, and also efficient high-altitude operation appears unlikely without some form of variable air inlet.

Previous experiments with auxiliary inlets have not included drag measurements which are necessary for a complete evaluation of net performance. Also, although pressure-recovery measurements have shown the advantages of using flow deflectors at high angles of attack, their effect on drag at low angles of attack has not been defined. The present investigation was initiated to determine the drag as well as pressure recovery and mass flow of a nose-inlet system at low angles of attack with both a flow deflector and an auxiliary inlet. It was the purpose of the investigation to use the experimental results to evaluate the over-all net performance of the inlet system for a variety of flight conditions on the basis of an effective-thrust ratio. Tests were conducted in the Ames 6- by 6-foot wind tunnel at Mach numbers up to 1.50 and in a range of Reynolds numbers per foot from 3.13×10^6 to 3.82×10^6 .

NOTATION

The following symbols are used in this report:

- A area, sq ft
- A_R reference area (body frontal area), 0.2394 sq ft
- a speed of sound, ft/sec

C_{D_N}	net drag coefficient, ¹ $\frac{D_N}{q_0 A_R} = (C_{D_T} - C_{D_I} - C_{D_B})$
C_{D_T}	total drag coefficient (balance drag measurement)
C_{D_I}	internal drag coefficient
C_{D_B}	base drag coefficient
C_F	effective-thrust ratio, $\frac{F_N - D_N}{F_{N_{isen}}}$
D_N	net drag, lb
F_N	net thrust, lb
$F_{N_{isen}}$	net thrust based on isentropic total pressure recovery, lb
h	operational altitude, ft
M	Mach number
M_1	equivalent entrance Mach number, $\frac{m_t}{\rho_1 A_1 a_1}$ (assumes isentropic flow relationships for the entrance station)
m_t	total mass-flow rate, $\rho_s V_s A_s$, slugs/sec
m_o	mass-flow rate based on inlet area, $\rho_o V_o A_1$, slugs/sec
P_t	total pressure, lb/sq ft
q	dynamic pressure, $\frac{1}{2} \rho V^2$, lb/sq ft
y	distance from center body surface, in.
V	velocity, ft/sec
α	angle of attack, deg
ρ	mass density, slugs/ft ³

¹In the past, this force has occasionally been referred to as external drag coefficient; it is herein termed net drag to emphasize its compatibility with net thrust.

~~CONFIDENTIAL~~

11

Subscripts

o	free stream
1	main-inlet entrance station
1a	auxiliary-inlet entrance station
2	outlet station of auxiliary duct
s	diffuser exit and compressor rake station
Exit	duct exit rake station

MODEL AND INSTRUMENTATION

A sketch of the basic test model and instrumentation is shown in figure 1. This model was also used for tests on several open-nose assemblies which are reported in reference 8. Details of one of the original open-nose assemblies (nose E) along with the additional assemblies which were tested in the present investigation are shown in figure 2.

Deflector extension D_I was approximately semielliptical in cross section perpendicular to the longitudinal axis with a flat undersurface set at a small angle to the free-stream direction ($1/2^\circ$). The edge of the deflecting surface was sharp. Deflector D_{II} was shaped by cutting back the leading edge of D_I approximately 0.65 inch at the tip and increasing the angularity of the undersurface to $6-1/2^\circ$. A sharp inlet lip profile was used with D_I while the lip used with D_{II} was blunted slightly (0.025-inch-radius model scale). These two lip profiles correspond to lips 1 and 2, respectively, of reference 8.

The design of auxiliary scoop A_I was such that the flow was turned abruptly upon entering the diffuser at station 1a; whereas the entrance to A_{II} was faired to turn the flow gradually. This fairing was accomplished by moving the entrance station forward. Each auxiliary-inlet area was approximately 12 percent of the main-inlet area of deflector D_I . A photograph showing the faired auxiliary scoop, A_{II} , mounted on nose assembly D is shown in figure 3. The cross-sectional-area variations of the diffusers which were tested are presented in figure 4. A comparison curve showing the area variation for a 1° equivalent conical diffuser is also included in figure 4.

Mass-flow ratios were controlled by a constant-speed vacuum pump and a valve located outside the wind tunnel. Mass-flow measurements

were made with an A.S.M.E. standard orifice meter. Drag measurements were made with a strain-gage balance which was mounted as shown in figure 1. The instrumentation rakes shown in figure 1 were used to measure pressure recoveries at both the compressor and exit stations, the exit measurements being necessary for the computation of internal drag. All calculation procedures are similar to those explained in reference 8.

TESTS AND DATA PRESENTATION

Tests were conducted on six configurations which are summarized in the table below using the symbol designations defined in the preceding section.

Nose assembly	Description
A	Sharp lip, $1/2^\circ$ deflector (D_I)
B	Round lip, $6-1/2^\circ$ deflector (D_{II})
C	Round lip, $6-1/2^\circ$ deflector (D_{II}), auxiliary scoop (A_I)
D	Round lip, $6-1/2^\circ$ deflector (D_{II}), faired auxiliary scoop (A_{II})
E	Basic inlet, round lip

Data for nose assembly E and the basic body, which were also investigated in reference 8, are presented for purposes of comparison. Tests were conducted at subsonic Mach numbers of 0, 0.7, 0.8, and 0.9 and at supersonic Mach numbers of 1.23, 1.35, and 1.50. Data were obtained for angles of attack of 0° and 5° at all test Mach numbers. The subsonic tests showed auxiliary scoop A_I to be inferior to A_{II} and, since the sharp turning angle of A_I would be even less desirable at higher speeds, nose C was omitted from tests at supersonic Mach numbers.

Total pressure measurements were made over a mass-flow-ratio range from 0.5 to maximum at a wind-tunnel stagnation pressure of 12 psia. Schlieren photographs were taken to record flow observations. In addition, schlieren observations during the tests gave qualitative information on flow steadiness. Final evaluation of the net performance of each nose configuration was obtained by computing effective-thrust ratios based on a J-57 engine operating at military rpm with full afterburning. The matching and optimizing procedure described in reference 8 was used to calculate the variation of effective-thrust ratio with Mach number for several representative flight schedules.

RESULTS AND DISCUSSION

Due to the multiple purpose of this investigation the following section has been subdivided for the sake of clarity. The first subsection concerns flow-deflector-inlet performance and compares the flow-deflector inlets to the basic open-nose inlet on the basis of pressure recovery, mass-flow ratio, and drag. In the second subsection, the auxiliary scoop is discussed by comparing characteristics of the flow-deflector auxiliary-scoop combinations to those of inlets with flow deflectors alone. Finally, an evaluation analysis is presented for both the flow-deflector and auxiliary-scoop inlets which is based on effective-thrust ratios.

Flow-Deflector-Inlet Performance

Pressure recovery and mass-flow ratio.- The static or simulated take-off condition is considered in figure 5 which presents total pressure recovery as a function of equivalent entrance Mach number. Nose A, which consisted of a sharp-edged deflector in combination with a sharp inlet lip, had both lower pressure recovery and lower maximum mass flow (lower maximum M_1) than nose E which was the basic open-nose inlet. Nose B which utilized a sharp-edged deflector and a slightly rounded duct lip also provided pressure recovery lower than nose E, but was within 2 percent of the basic inlet over the complete range of entrance Mach numbers. The maximum values of M_1 were 0.56 and 0.57 for noses B and E, respectively.

The total pressure recovery, as a function of mass-flow ratio, is presented for subsonic Mach numbers in figure 6. In figure 6(a), for $\alpha = 0^\circ$, the flow-deflector inlets and the basic inlet show almost identical variation of pressure recovery with mass-flow ratio. A comparison of the data in figure 6(b) with that of figure 6(a) shows there was no change in pressure recovery due to increasing the angle of attack of nose B from 0° to 5° . This was also shown to be true for the basic inlet in reference 8.

Pressure-recovery and mass-flow curves for supersonic Mach numbers are presented in figure 7. For $\alpha = 0^\circ$, figure 7(a), the pressure recovery and maximum mass-flow ratio were considerably less for nose A than for nose E. In addition, on the basis of schlieren observations at $M_\infty = 1.50$, nose A could not maintain steady internal-flow operation at subcritical mass-flow ratios. This unsteadiness might also be expected on the basis of the positive slope of the curve for nose A in figure 7(a).

Modifications were made to the deflecting surface and inlet lip profile of nose A (see Model and Instrumentation) in an attempt to improve the inlet characteristics. The angularity of the deflector undersurface was increased since the data for nose A (fig. 7) showed that the pressure recovery improved at angles of attack as a result of reduced shock losses. Also, it was expected that the increased angularity would improve the flow steadiness by reducing both the normal-shock-wave intensity and the growth of boundary layer on the deflector surface. The pressure recovery and maximum mass-flow ratio of the modified inlet, nose B, surpassed nose E at Mach numbers of 1.35 and 1.50 (fig. 7(a)). At $M_\infty = 1.50$, the critical pressure recovery² for nose B was 0.90 and the maximum mass-flow ratio was 1.07. Corresponding values measured for nose E were 0.87 and 1.03, respectively. Also, at $M_\infty = 1.50$ steady operation was maintained with nose B at all mass-flow ratios above about 0.85. As shown in figure 7(b), increasing the angle of attack to 5° improved nose A more than nose B, although nose B remained superior at all Mach numbers except 1.23. Reference 8 indicates that a similar change in angle of attack for nose E would produce no significant effect.

Pressure-recovery profiles are presented in figure 8 and show that nose B reduced the circumferential variation in pressure recovery near the outer duct wall which was in evidence for nose E.

Net drag coefficient.- The net drag characteristics at subsonic and supersonic speeds are shown in figure 9. The net drag measurements showed considerable scatter at subsonic speeds and, consequently, faired curves are presented in figure 9(a) for qualitative comparison only. These curves indicate that the drag for a deflector inlet can be considerably greater than the drag for a basic open-nose inlet. The disturbances caused by the juncture of the duct lips and the flat undersurface of the deflector probably contributed to the drag increase. The large drag differences that occurred between the two deflectors are not readily explainable, but the questionable nature of the data does not justify any positive conclusion regarding the magnitude of the subsonic drags. However, the evaluation analysis is considered reliable since at subsonic speeds the effective-thrust ratio is relatively insensitive to drag.

At supersonic speeds, figure 9(b) shows that at maximum mass-flow ratio, the drag of nose A was approximately equal to the drag of nose E; whereas the drag of nose B was about 10 percent higher than that for nose E. The increase in drag of nose B is believed to be principally wave drag resulting from the stronger oblique shock wave originating from the under surface of the deflector. This explanation can also be applied to the results presented in figure 9(c). These results show that increasing the angle of attack to 5° increased the drag of both

²Critical pressure recovery is defined as the maximum pressure recovery at maximum mass-flow ratio.

deflector inlets about 10 percent at the maximum mass-flow ratio. Data in reference 8 indicate the basic inlet would undergo a greater percent increase in drag under the same conditions.

Auxiliary-Scoop Performance

Pressure recovery and mass-flow ratio.-- Installation of an auxiliary scoop increased the pressure recovery of the deflector inlet at static conditions (fig. 5). The pressure recovery of nose D at an entrance Mach number of 0.55 was 5 percent and 3 percent higher than that for noses B and E, respectively. Changing the auxiliary-scoop geometry to the type tested with nose C showed only small effects on performance at static conditions.

At subsonic speeds figure 6(a) shows that auxiliary scoops increased the maximum mass-flow ratio approximately 10 percent or slightly less than the proportional increase in intake area represented by the auxiliary-scoop area (12 percent). This difference was probably due to the body boundary layer forward of the auxiliary scoop. The data in figure 6(b) show there was no effect due to increasing the angle of attack to 5°.

At supersonic speeds, auxiliary scoop A_{II} increased the maximum mass-flow ratio in a manner similar to that at subsonic speeds (fig. 7(a)). Unlike the subsonic effect, however, total pressure recovery was reduced at supersonic speeds by use of the auxiliary scoop. As might be expected, further reduction occurred with increasing Mach numbers due to adverse shock-wave boundary-layer interaction effects forward of the auxiliary scoop. This interaction is evident in the flow patterns associated with nose assemblies B and D which are shown by schlieren photographs in figure 10.³ The major effect of increasing the angle of attack to 5° was an increase in maximum mass-flow ratio of about 4 percent at $M_0 = 1.50$ (fig. 7(b)).

The pressure-recovery profiles in figure 8 show no appreciable increase in the circumferential pressure-recovery variation due to the auxiliary scoop, but some reduction in pressure recovery did occur along the center body.

Net drag coefficient.-- A comparison of the results from noses B and D in figure 9(a) shows that the auxiliary scoop caused the drag to increase about 65 percent at $M_0 = 0.70$ and about 50 percent at $M_0 = 0.90$. The faired auxiliary scoop, A_{II} (nose D), had lower drag than scoop A_I (nose C).

³The circular striations in the photographs are due to nonuniformity of the glass in the test-section window.

At supersonic speeds, figure 9(b) shows the auxiliary scoop, AII, increased the drag about 0.015 (10 percent) at the maximum mass-flow ratio at all three Mach numbers. The reason for the rather large drag increases due to the auxiliary scoop is evident in figure 10. Schlieren photographs show the regions of disturbed boundary layer which existed rearward of the auxiliary scoop. Increasing the angle of attack to 5° increased the drag of nose D about 10 percent at $M_0 = 1.23$ for the maximum mass-flow-ratio condition, but the drag increase was less than 5 percent at $M_0 = 1.50$.

Evaluation Analysis

Design inlet area.- The effective-thrust-ratio parameter $F_N - D_N / F_{Nisen}$ combines the three basic inlet characteristics, that is, pressure recovery, mass-flow ratio, and drag, into a single figure of merit by which inlet systems can be evaluated. For fixed-inlet systems an evaluation based on a specific flight schedule is very sensitive to the design inlet area. The effect of inlet area on the effective-thrust ratio is shown in figure 11 for two representative Mach numbers at an operating altitude of 35,000 feet. The general nature of these curves would not be changed for other altitudes. At a Mach number of 1.50 the curves drop off rapidly on both sides of the peak design values. The drop at high values of inlet area results from reduced mass-flow-ratio operation which is accompanied by increases in net drag due to the additive-drag component and slight reductions in pressure recovery (see figs. 7(a) and 9(b)). At low values of inlet area the inlet operates supercritically at greatly reduced values of pressure recovery. By comparison, the curves for a Mach number of 0.80 again show rapid reductions in effective-thrust ratio at low inlet areas due to insufficient engine air flow; however, reduced mass-flow operation at large inlet areas shows relatively no effect. The slight drag increase at this operating condition is compensated for by a rise in pressure recovery (see figs. 6(a) and 9(a)). The inlet area for peak performance at $M_0 = 1.50$ would provide a value of effective-thrust ratio at $M_0 = 0.80$ which would be considerably less than maximum. This fact points out the importance of judicious selection of inlet area for the design area of a fixed system. The design selection must be dictated by the intended operating schedule of the aircraft, since it is impossible to select a single area which will give peak performance at all conditions of Mach number and altitude. Design areas for a Mach number of 1.50 at 35,000 feet are shown on the curves in figure 11.

Flow deflector.- The isolated effect of a flow deflector on the net performance of an open-nose inlet is shown in figure 12 by comparing the results from nose assemblies A, B, and E. For a fixed inlet area based on a design Mach number of 1.50 at 35,000 feet, the evaluation shows

deflector D_I (nose A) would give considerably lower performance than the basic open-nose inlet over the entire Mach number range for the two altitudes considered in the analysis. Nose B, however, would give performance very close to that of nose E at all Mach numbers and actually surpass nose E performance above $M_0 = 1.30$ at the design altitude (35,000 feet). The reference curve of effective-thrust ratio shown in figure 12 is based on normal-shock-wave pressure recovery combined with the drag of the basic body. As shown in figure 12, the reference curve is equaled by nose B at Mach numbers greater than 1.40 at an altitude of 35,000 feet.

On the basis of figure 12, it can be concluded that very little difference exists between the net performance attainable with a deflector inlet and that of an open-nose inlet at low angles of attack. At Mach numbers up to 1.30 the basic inlet is slightly superior for the design altitude; whereas above $M_0 = 1.30$ the deflector is beneficial. Any final selection of inlet type would require consideration of the performance of the deflector inlet at angles of attack as well as its flow steadiness characteristics at supersonic speeds below a mass-flow ratio of 0.85.

Auxiliary scoop.- It has been shown that opening an auxiliary scoop has adverse effects on the pressure recovery and drag of an open-nose air-inlet system. Such a scoop would provide increases in mass flow and, therefore, its only application would be to supplement the main inlet under supercritical flow conditions (compare noses B and D in fig. 11). A nose-inlet system consisting of an auxiliary scoop in conjunction with a deflector nose inlet is evaluated in figure 13. A range of Mach numbers is considered at two altitudes so as to determine the effect of the auxiliary scoop on over-all performance for representative operating schedules. The effective-thrust ratio as a function of M_0 is shown in figure 13(a) for a design Mach number of 1.50 and a design altitude of 35,000 feet. A comparison between noses B and D operating at 35,000 feet shows the auxiliary scoop would be beneficial below a Mach number of 0.95 but should be completely closed at all higher speeds. At Mach numbers of 0.80 and 1.50 in figure 13(a) effective-thrust ratios are presented for an inlet system with the auxiliary-scoop area increased to 24 percent of the main inlet area. These data were obtained by linear extrapolation of the pressure recovery, mass-flow ratio, and drag measurements of noses B and D and are considered to be conservative. Figure 13(a) shows that very little gain would be experienced at $M_0 = 0.80$ by increasing the auxiliary-scoop area. For Mach numbers below 0.80 the inlet area required to satisfy the turbojet engine would be increased and, consequently, either size of auxiliary scoop would be beneficial.

Results shown in figure 11 indicate that a design inlet area for $M_0 = 1.50$ would be considerably less than the area for maximum performance at $M_0 = 0.80$. For comparison purposes the effective-thrust ratios

for a flow-deflector inlet oversized by 12 percent are plotted in figure 13 ($B + 0.12 A_1$). The oversized inlet area corresponds to the optimum value required for a design Mach number of about 0.90. The thrust comparison for an altitude of 35,000 feet in figure 13(a) shows a considerable gain in performance at Mach numbers up to 1.25 due to oversizing the inlet; whereas performance is lost at speeds above this value. On the basis of these results, any decision as to the most efficient inlet system for operation at Mach numbers up to 1.50 would necessarily be dependent upon the most critical speed range for a particular design and also on the added weight and complexity resulting from an auxiliary-scoop installation.

The curves in figure 13(a) for an operating altitude of 15,000 feet show that an auxiliary scoop or an oversized inlet would reduce the effective-thrust ratio over most of the Mach number range. This can be explained by the fact that engine air-flow requirements are reduced at altitudes less than the design altitude and, therefore, increasing the inlet area is not beneficial.

The effective-thrust ratio as a function of flight Mach number for a design Mach number of 1.50 at a design altitude of 15,000 feet, as might be required of low-altitude attack aircraft, is shown in figure 13(b). The auxiliary scoop and the oversized inlet both show a large improvement in performance over that of nose B at an operating altitude of 35,000 feet since the inlet-area requirements are greater than at the design altitude. Under this condition the auxiliary scoop would be open throughout the speed range, and at a Mach number of 0.80 a 24-percent auxiliary area would give higher performance than the oversized nose B. However, at $M_0 = 1.50$ the performance of the auxiliary scoop would be slightly inferior to the fixed oversized inlet.

For operation at the design altitude of 15,000 feet, the auxiliary scoop is useful at Mach numbers below 1.25. The data indicate that provided a large auxiliary scoop ($0.24 A_1$) was utilized, an auxiliary-scoop system could operate more efficiently than the fixed oversized inlet up to a Mach number of approximately 1.10 and in the closed position would be superior above $M_0 = 1.35$.

The following table summarizes the effect of an auxiliary scoop and a fixed oversized inlet on the net thrust of an open-nose air-inlet system. The thrust ratios tabulated for the variable auxiliary inlet are the highest values which could be obtained with either of the two auxiliary scoop sizes ($0.12 A_1$ and $0.24 A_1$) or with inlet B.

Design conditions	Operational conditions	Effective-thrust ratio, C_F		
		Fixed oversized inlet (B+0.12 A ₁)	Variable auxiliary inlet (B,D, or D+)	Fixed inlet (B)
$M_\infty = 1.50$ at 15,000 ft	0.80 at 15,000 ft	0.800	0.825	0.665
	1.50 at 15,000 ft	.435	.465	.465
	.80 at 35,000 ft	.695	.730	.570
	1.50 at 35,000 ft	.580	.560	.480
$M_\infty = 1.50$ at 35,000 ft	.80 at 15,000 ft	.900	.900	.900
	1.50 at 15,000 ft	.330	.370	.370
	.80 at 35,000 ft	.915	.880	.850
	1.50 at 35,000 ft	.585	.620	.620

This summary table alone does not provide a basis for any conclusion regarding the necessity of using auxiliary-inlet systems, since any conclusion regarding use of auxiliary inlets also depends upon the aircraft flight plan and engine air-flow requirements as well as the design details of the actual auxiliary-inlet installation.

CONCLUSIONS

Conclusions resulting from an investigation of flow deflectors and auxiliary scoops combined with a nose air inlet are as follows:

1. The pressure recovery of a deflector inlet at static conditions was slightly less (within 2 percent) than that of the basic open-nose inlet; whereas the auxiliary scoop provided an increase in pressure recovery at this condition.
2. The net performance attained with a deflector inlet, which improves performance at angles of attack, was essentially the same as that for a basic open-nose inlet at low angles of attack. The deflector, however, was found to have less desirable flow-steadiness characteristics than those of the basic inlet.
3. The auxiliary-scoop inlet increased the maximum mass-flow ratio at all Mach numbers in proportion to the increase in entrance area represented by the auxiliary scoop; however, pressure recovery was slightly reduced and drag was increased.
4. On the basis of effective-thrust ratios it is indicated that the variable auxiliary inlet can be advantageous for certain flight applications in which it is required to operate over a wide range of Mach numbers and altitudes. Any conclusion regarding the specific use of

auxiliary inlets will depend on the aircraft flight schedule and the design details of the actual auxiliary-inlet installation.

Ames Aeronautical Laboratory
National Advisory Committee for Aeronautics
Moffett Field, Calif., May 6, 1954

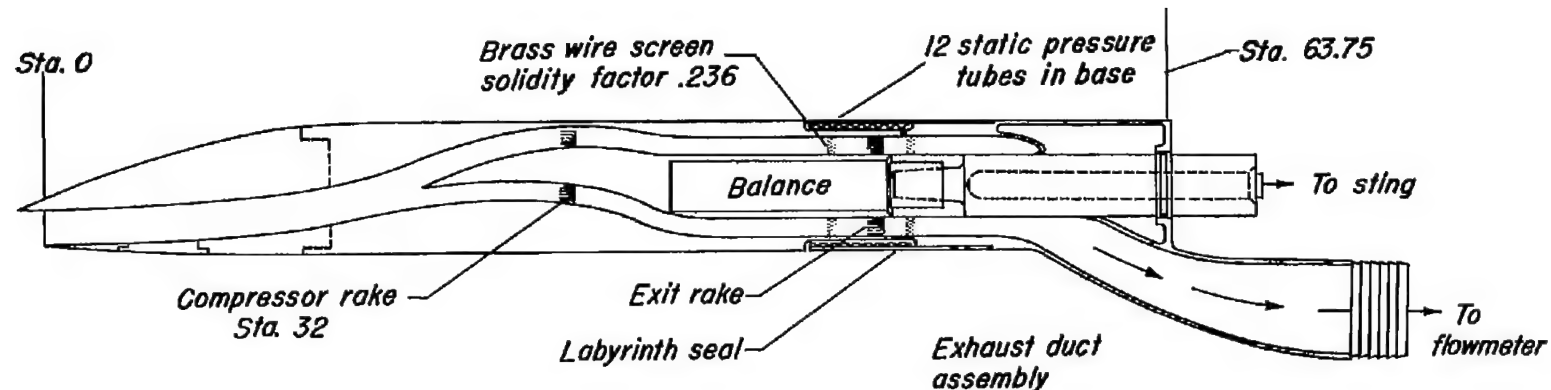
REFERENCES

1. Leissler, L. Abbott, and Hearth, Donald P.: Preliminary Investigation of Effect of Angle of Attack on Pressure Recovery and Stability Characteristics for a Vertical-Wedge-Nose Inlet at Mach Number of 1.90. NACA RM E52E14, 1952.
2. Beheim, Milton A.: A Preliminary Investigation at Mach Number 1.91 of an Inlet Configuration Designed for Insensitivity to Positive Angle-of-Attack Operation. NACA RM E53E20, 1953.
3. Beheim, Milton A.: A Preliminary Investigation at Mach Number 1.91 of a Diffuser Employing a Pivoted Cone to Improve Operation at Angle of Attack. NACA RM E53I30, 1953.
4. Carter, Howard S., and Merlet, Charles F.: Preliminary Investigation of the Total-Pressure-Recovery Characteristics of a Symmetric and an Asymmetric Nose Inlet over a Wide Range of Angle of Attack at Supersonic Mach Numbers. NACA RM L53J30, 1953.
5. Allen, J. L., and Beke, Andrew: Performance Comparison at Supersonic Speeds of Inlets Spilling Excess Flow by Means of Bow Shock, Conical Shock or Bypass. NACA RM E53H11, 1953.
6. Scherrer, Richard, Stroud, John F., and Swift, John T.: Preliminary Investigation of a Variable-Area Auxiliary Air-Intake System at Mach Numbers From 0 to 1.3. NACA RM A53A13, 1953.
7. Brajnikoff, George B., and Stroud, John F.: Experimental Investigation of the Effect of Entrance Width-to-Height Ratio on the Performance of an Auxiliary Scoop-Type Inlet at Mach Numbers From 0 to 1.3. NACA RM A53E28, 1953.
8. Mossman, Emmet M., and Anderson, Warren E.: The Effect of Lip Shape on a Nose-Inlet Installation at Mach Numbers From 0 to 1.5 and a Method for Optimizing Engine-Inlet Combinations. NACA RM A54B08, 1954.

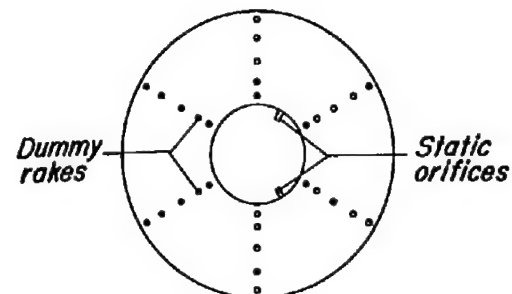
CONFIDENTIAL

14

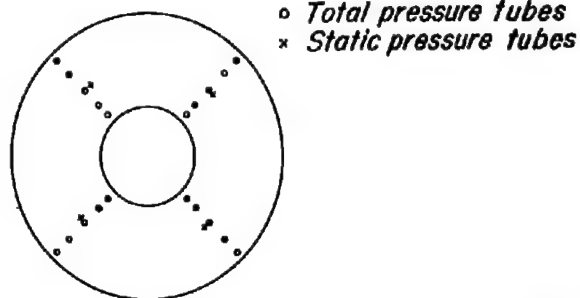
NACA RM A54E06



Dimensions:
Length = 63.75 in.
Maximum diameter = 6.62 in.



Compressor rake looking aft.



Exit rake looking aft.



Figure 1.- Sketch of air-induction model.

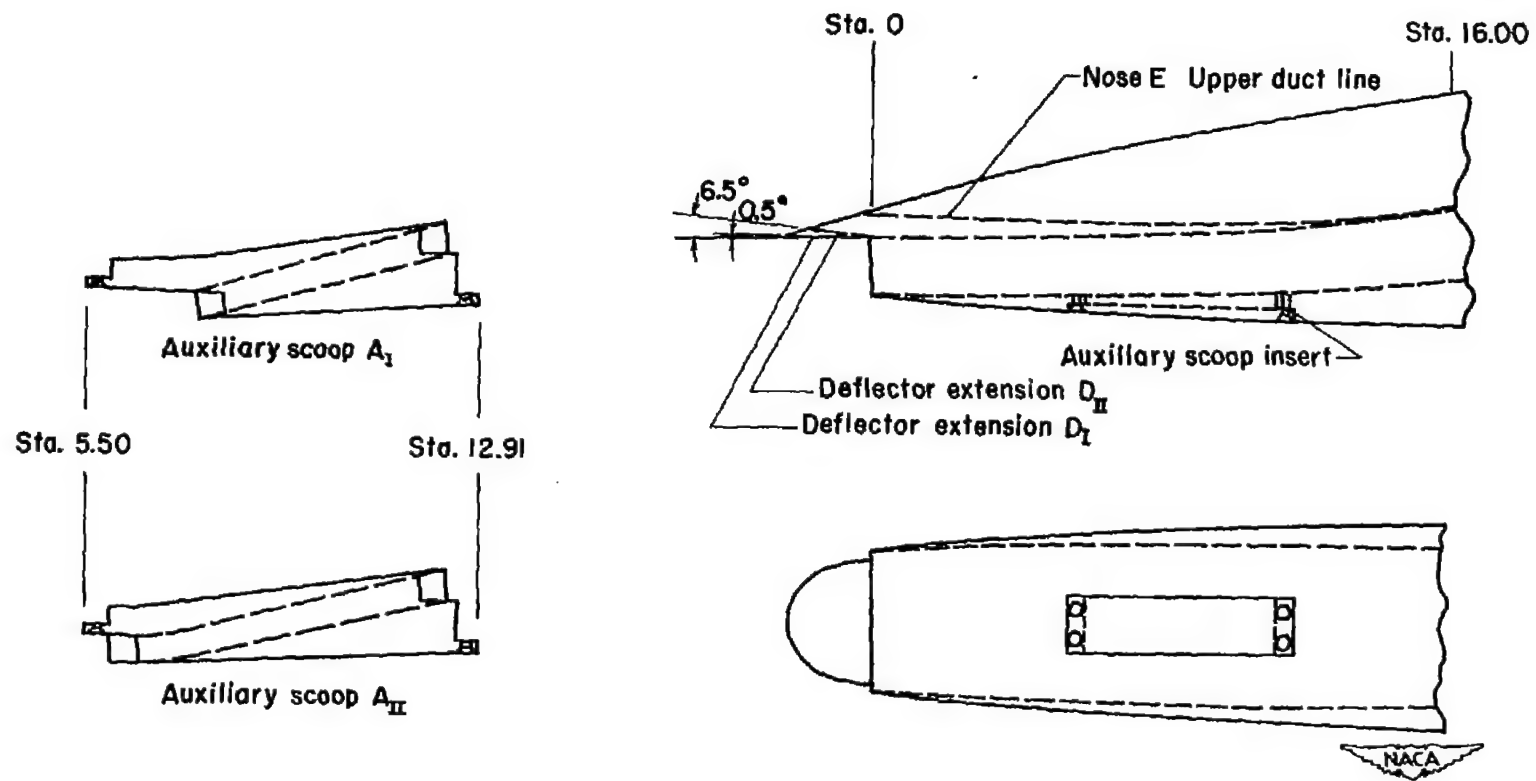
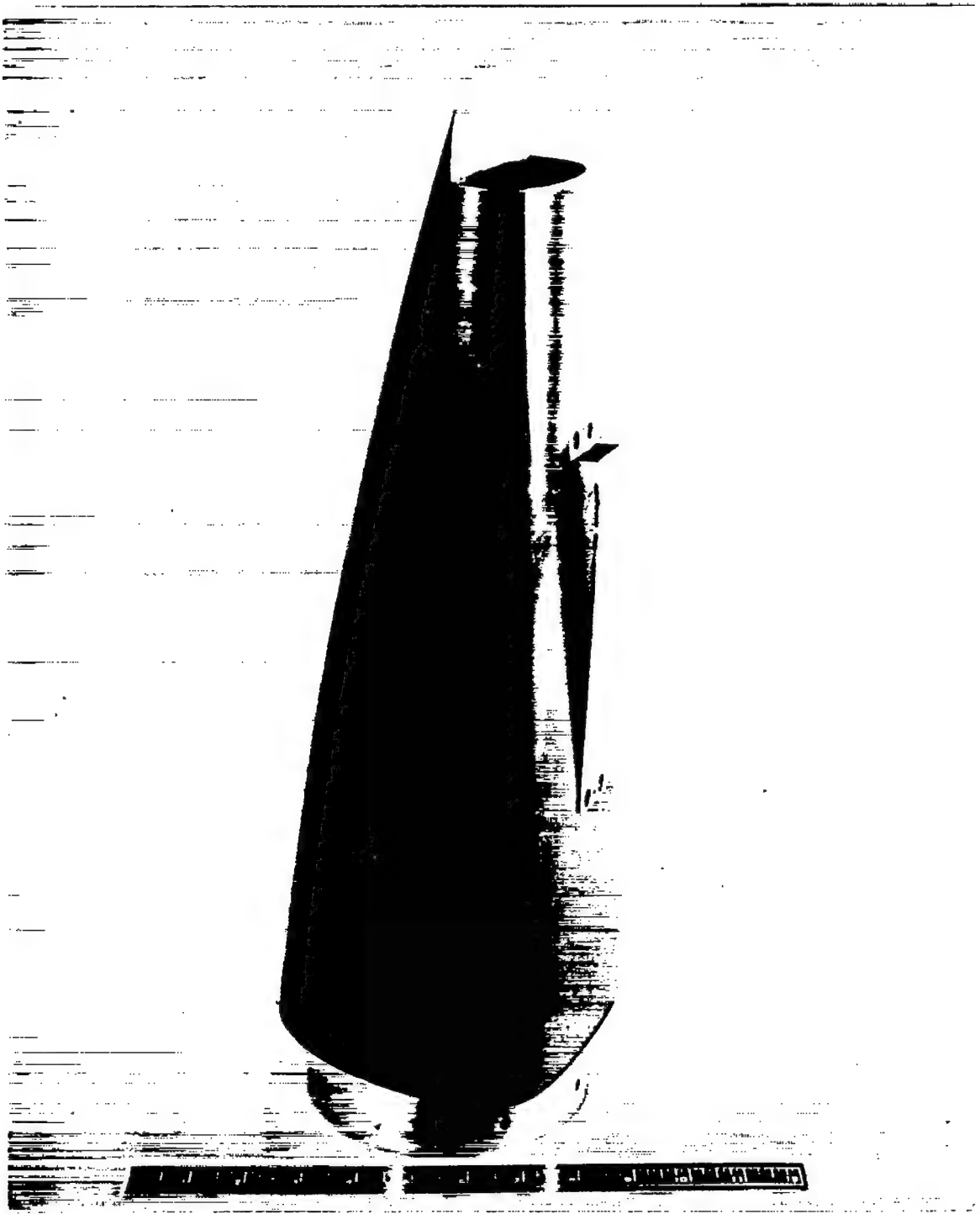


Figure 2.- Sketch of deflector nose assemblies and auxiliary scoops.



A-19009

Figure 3.- Photograph of nose assembly D showing deflector D_{II} and auxiliary scoop A_{III}.

CONFIDENTIAL

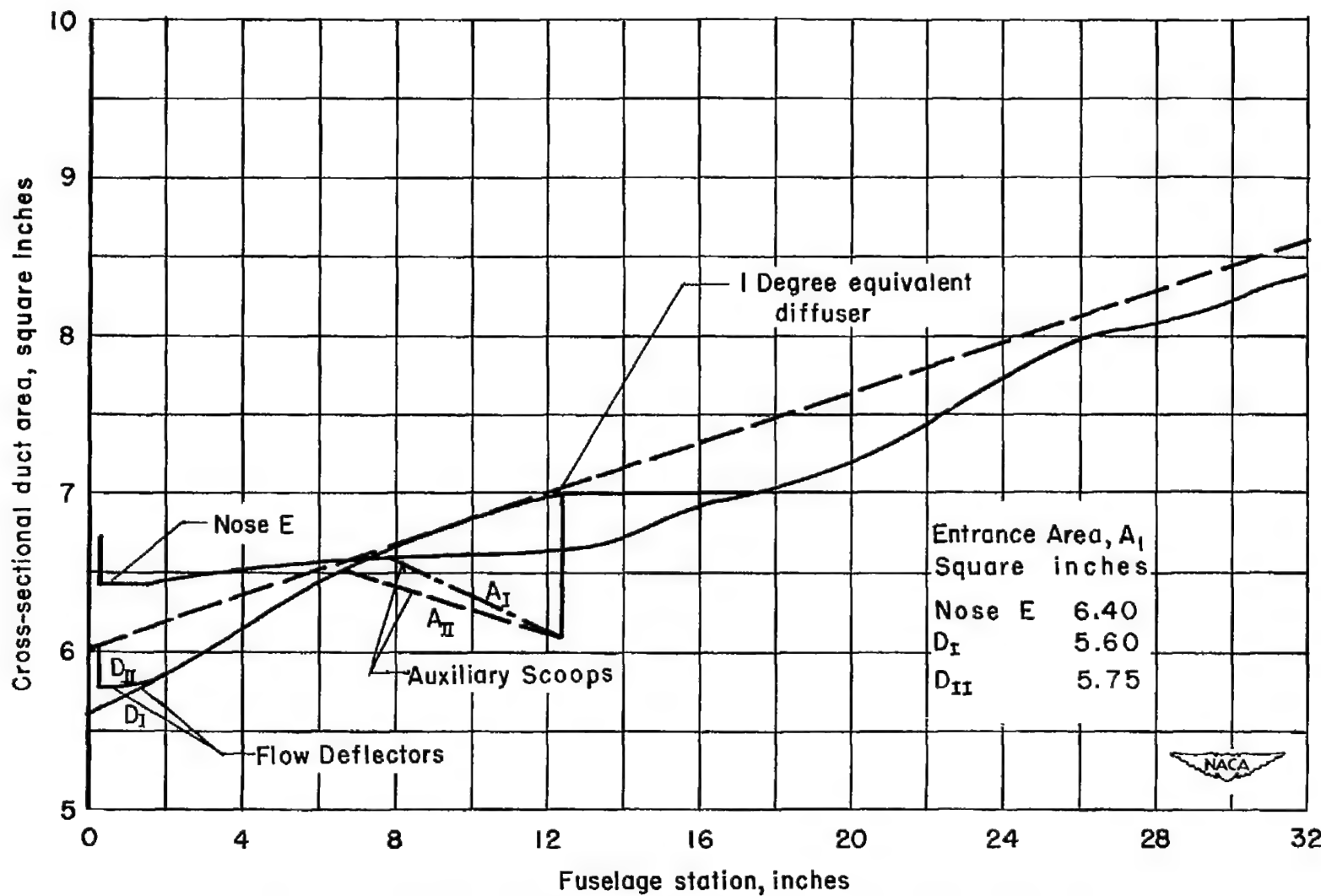


Figure 4.- Diffuser area variation for several test nose assemblies.

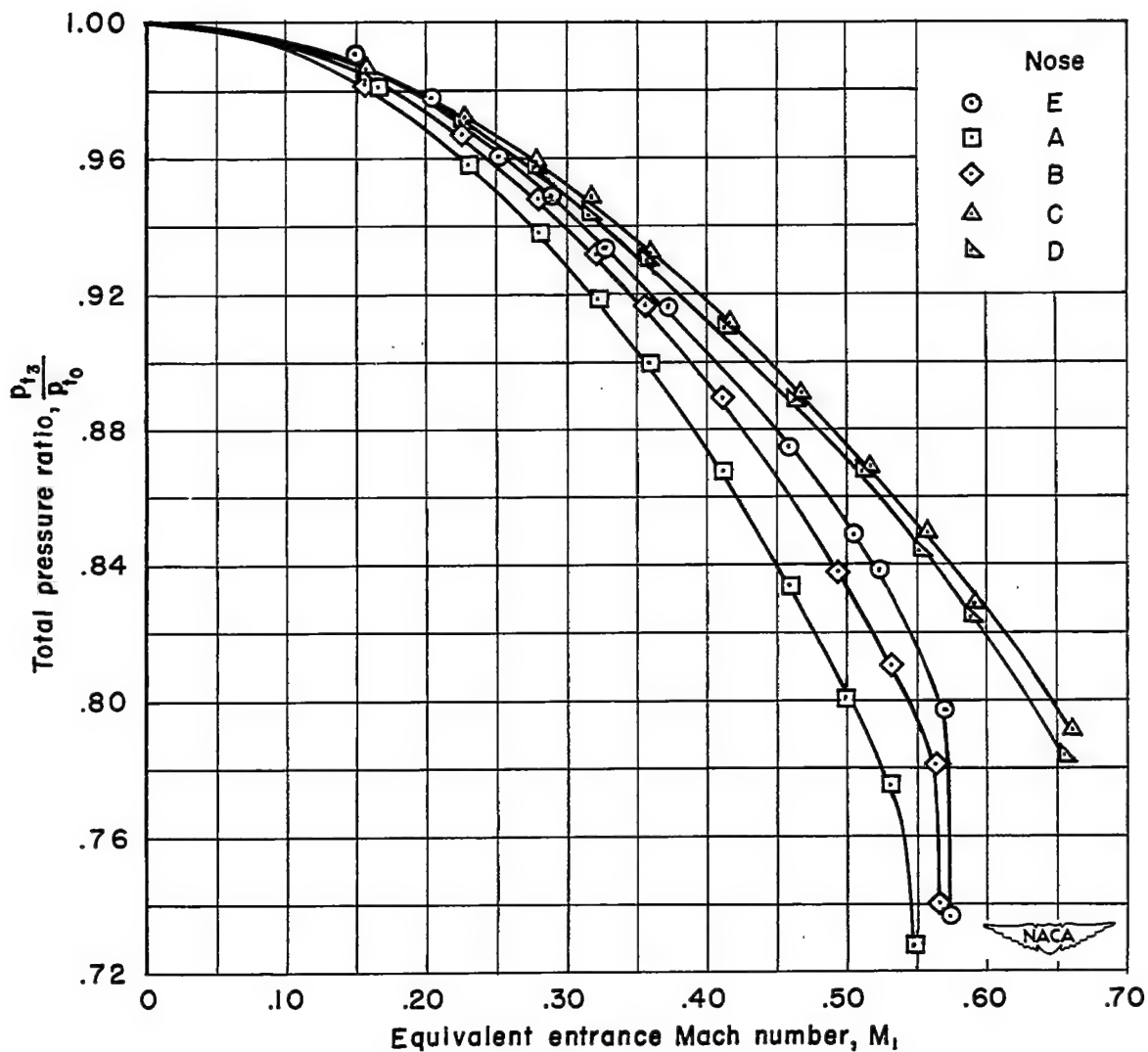


Figure 5.- A comparison of total pressure ratio and entrance Mach number characteristics of several nose assemblies at static conditions.

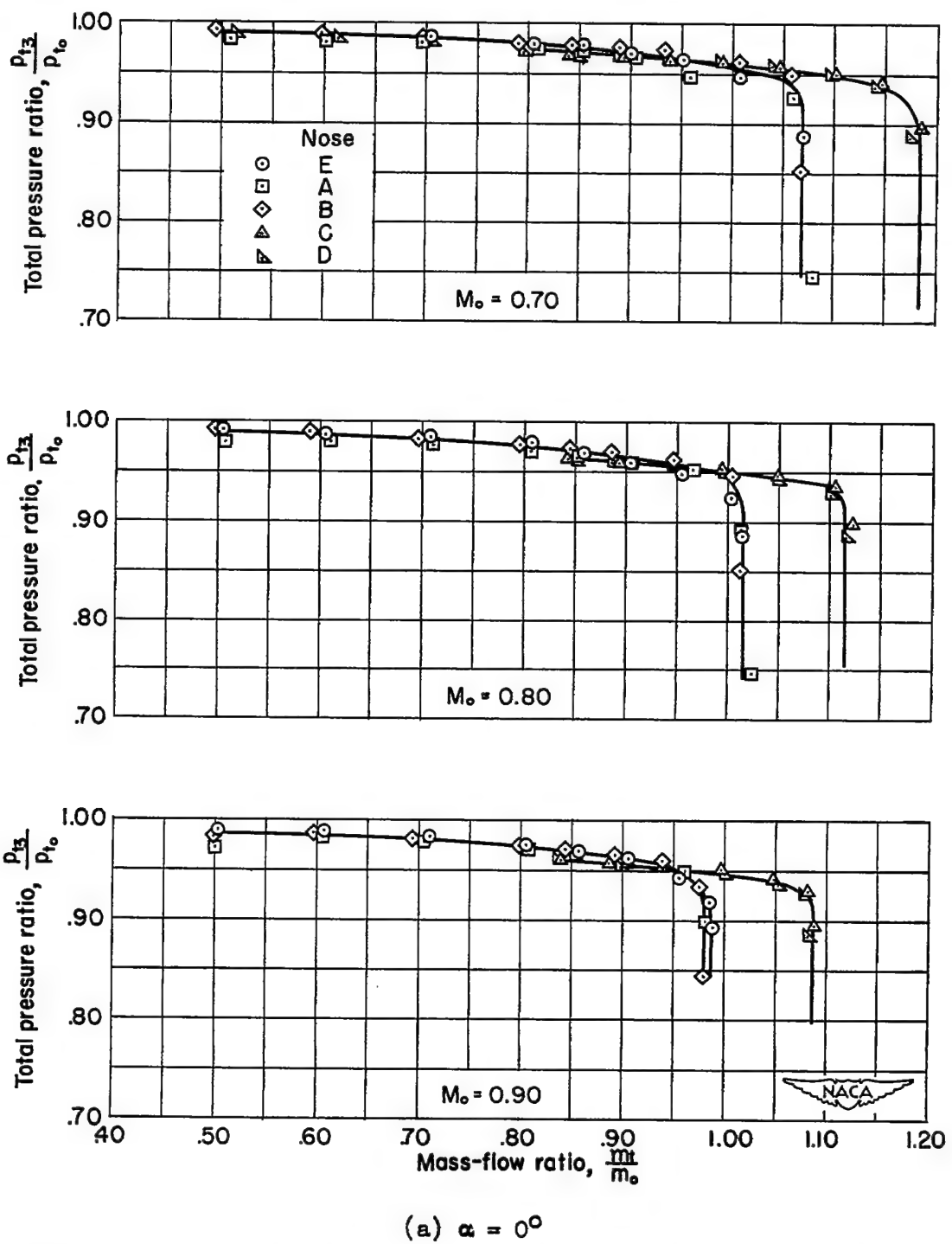


Figure 6.- A comparison of the pressure recovery and mass-flow ratio characteristics of several nose assemblies at subsonic Mach numbers.

CONFIDENTIAL

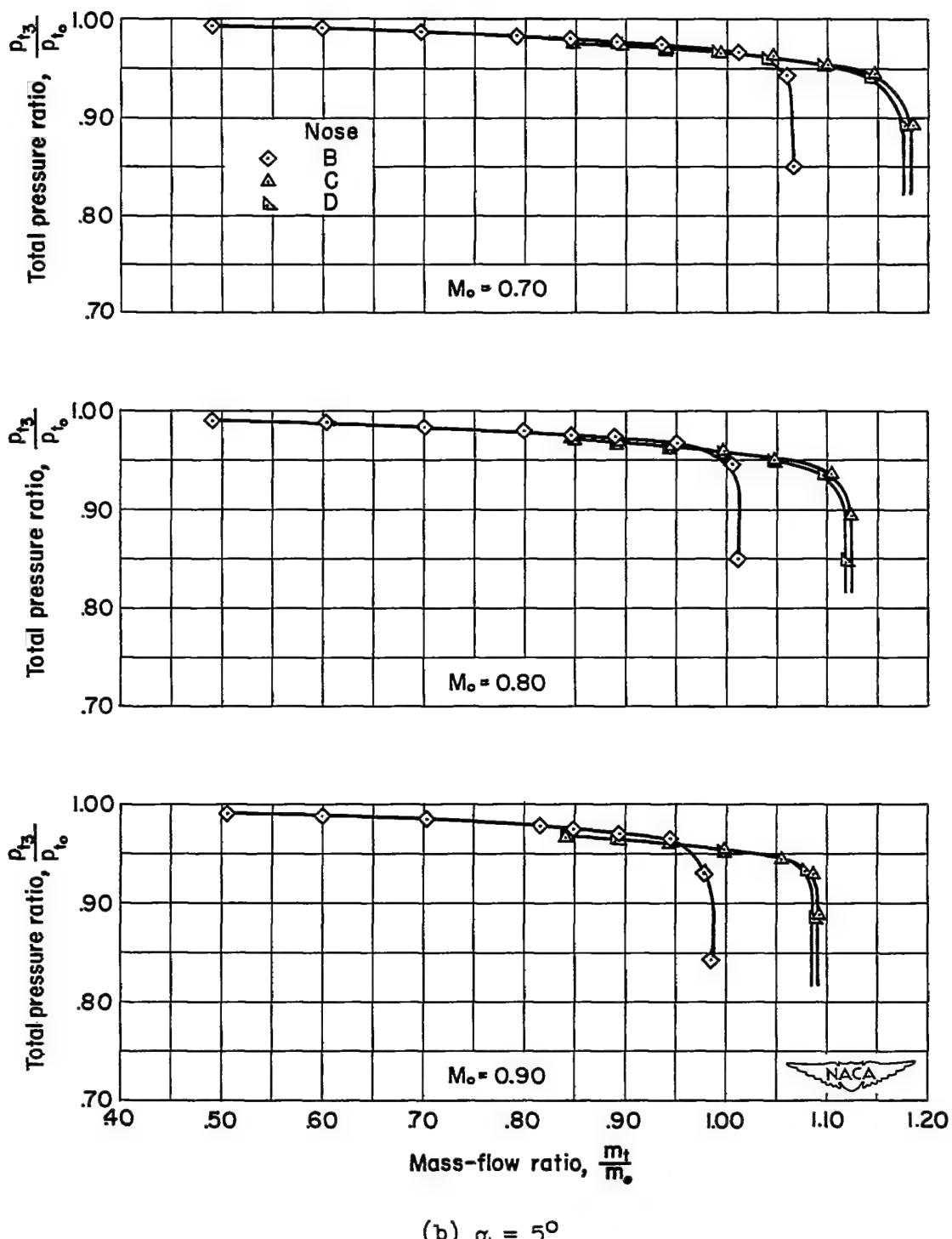
(b) $\alpha = 5^\circ$

Figure 6.- Concluded.

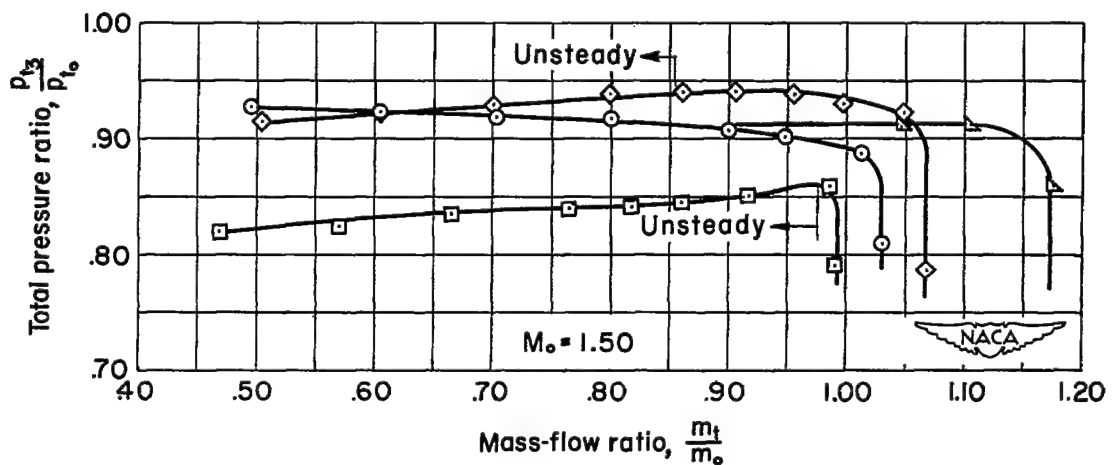
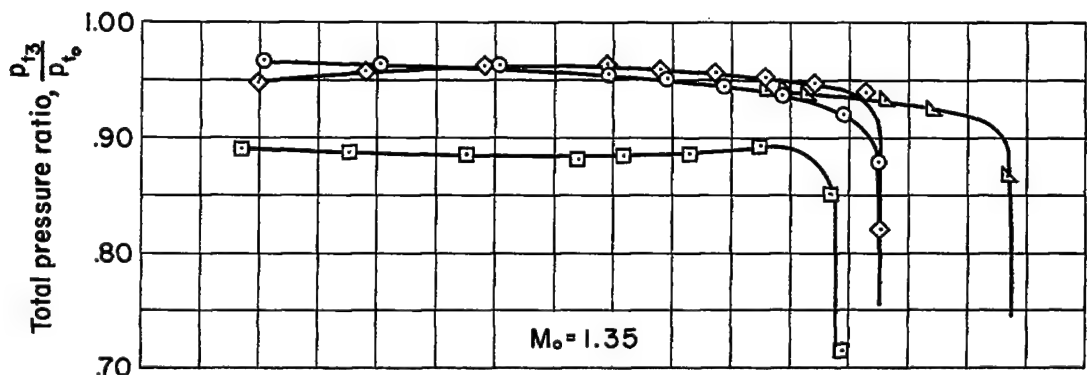
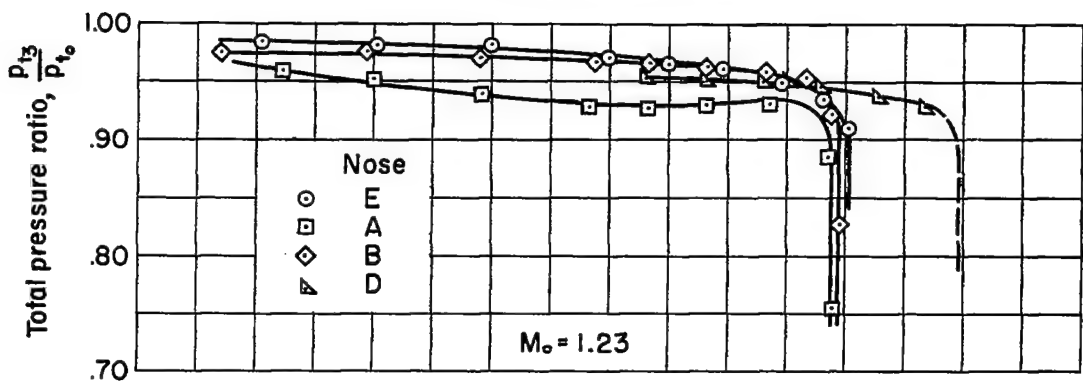
(a) $\alpha = 0^\circ$

Figure 7.- A comparison of the pressure recovery and mass-flow ratio characteristics of several nose assemblies at supersonic speeds.

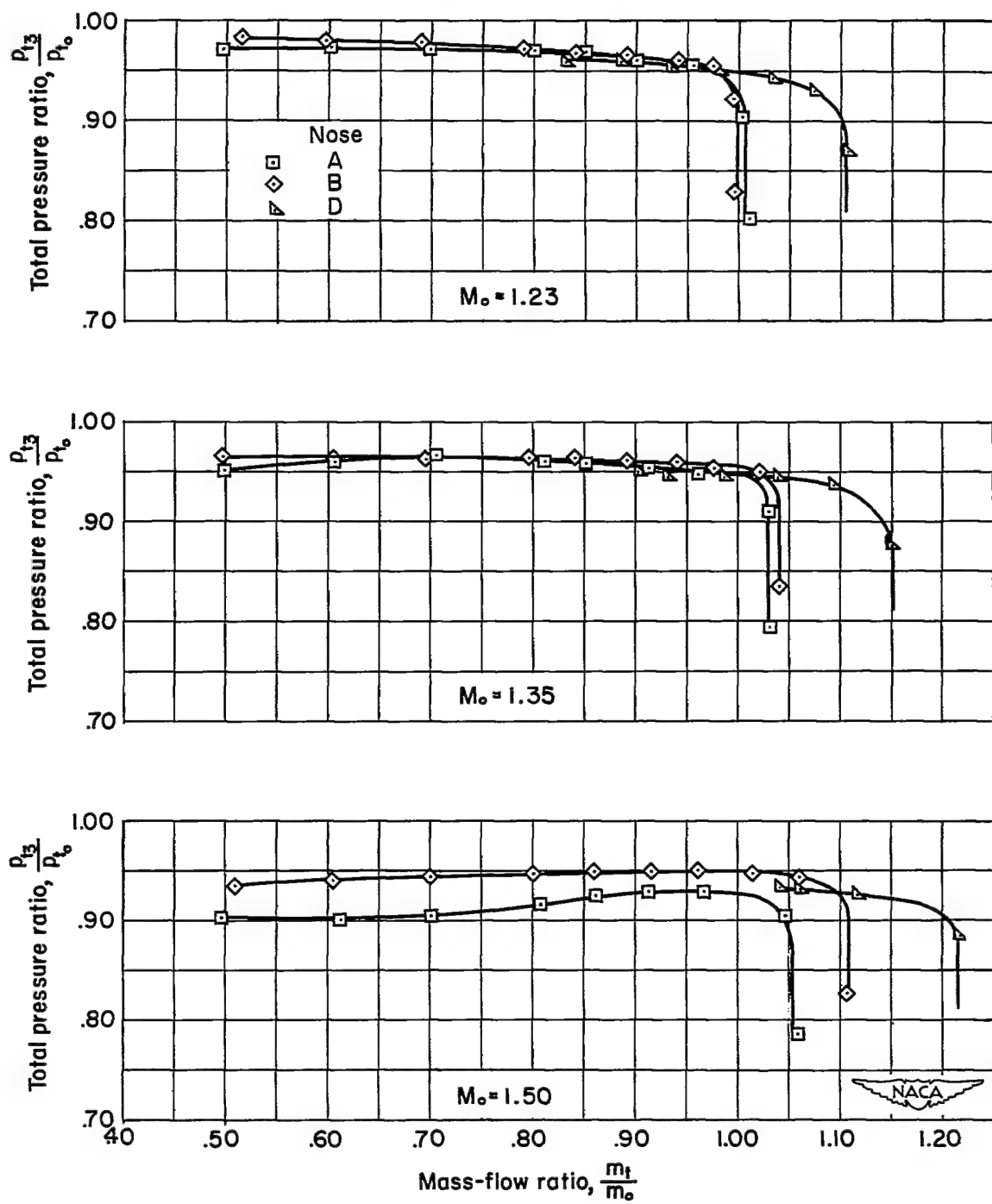
(b) $\alpha = 5^\circ$

Figure 7.- Concluded.

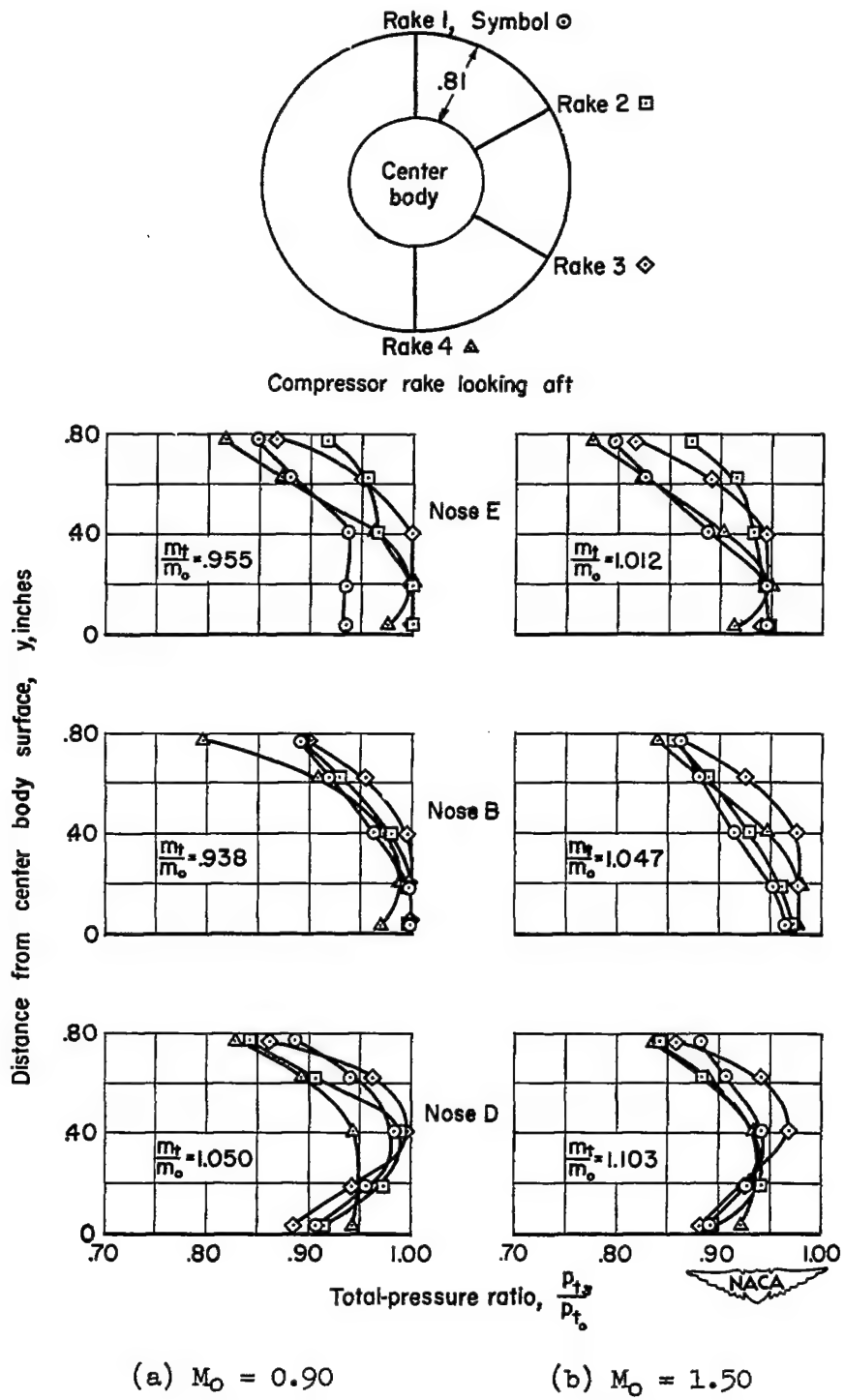
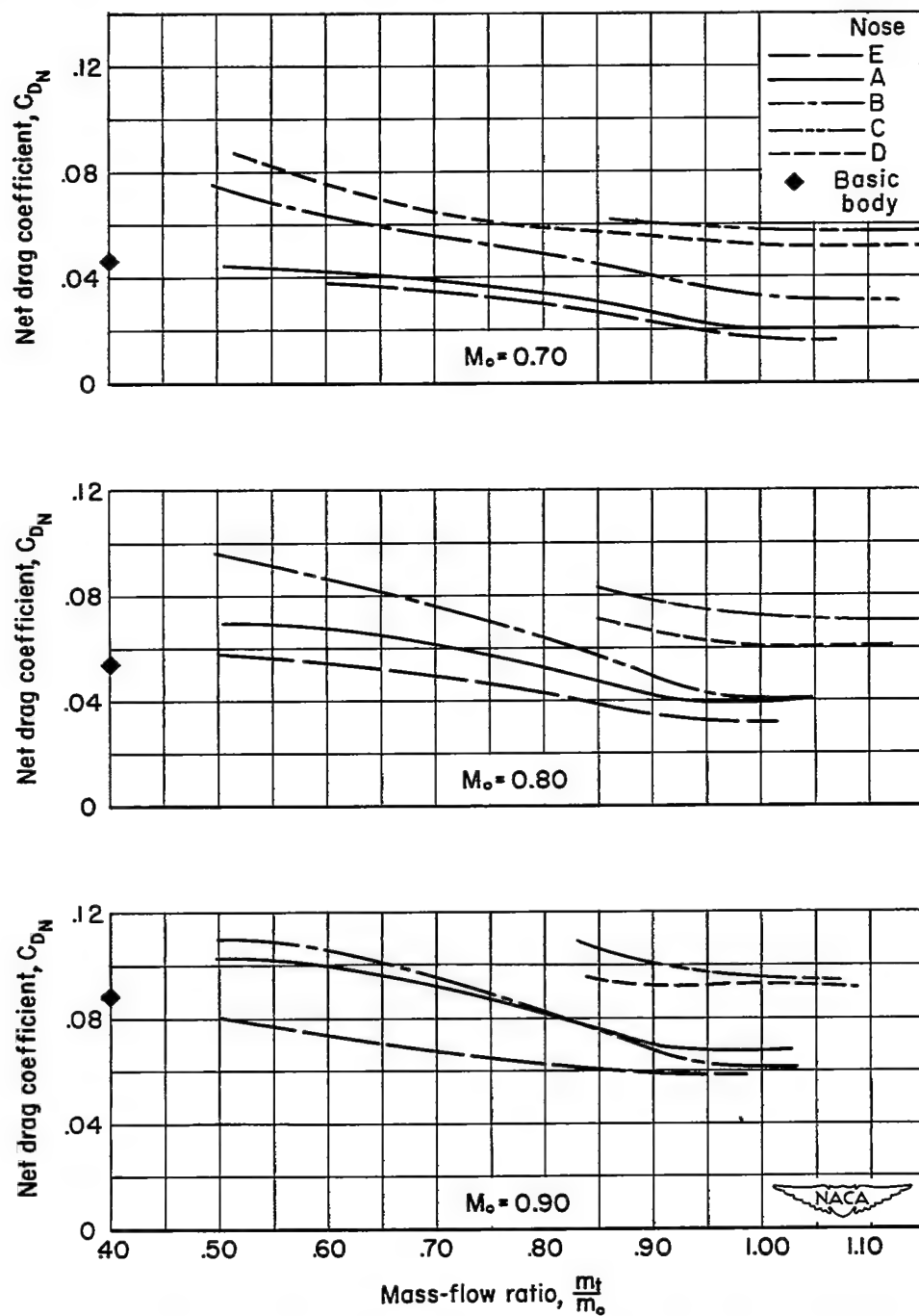


Figure 8.- A comparison of total pressure recovery profiles at the compressor station. Approximately critical pressure recovery, $\alpha = 0^\circ$.

~~CONFIDENTIAL~~



(a) Subsonic Mach numbers, $\alpha = 0^\circ$ (approximate values)

Figure 9.- A comparison of the net drag characteristics of several nose assemblies.

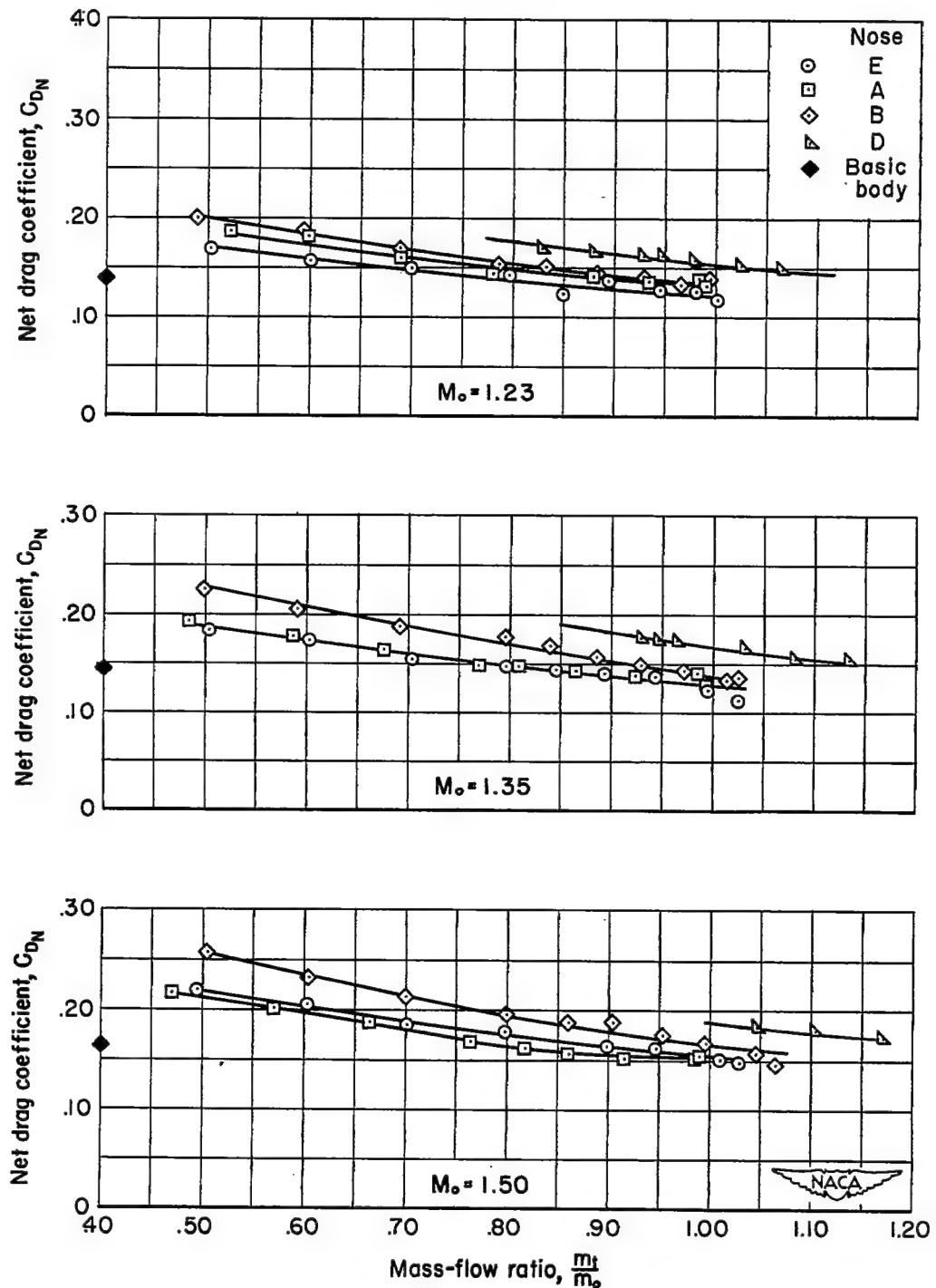
(b) Supersonic Mach numbers, $\alpha = 0^\circ$

Figure 9.- Continued

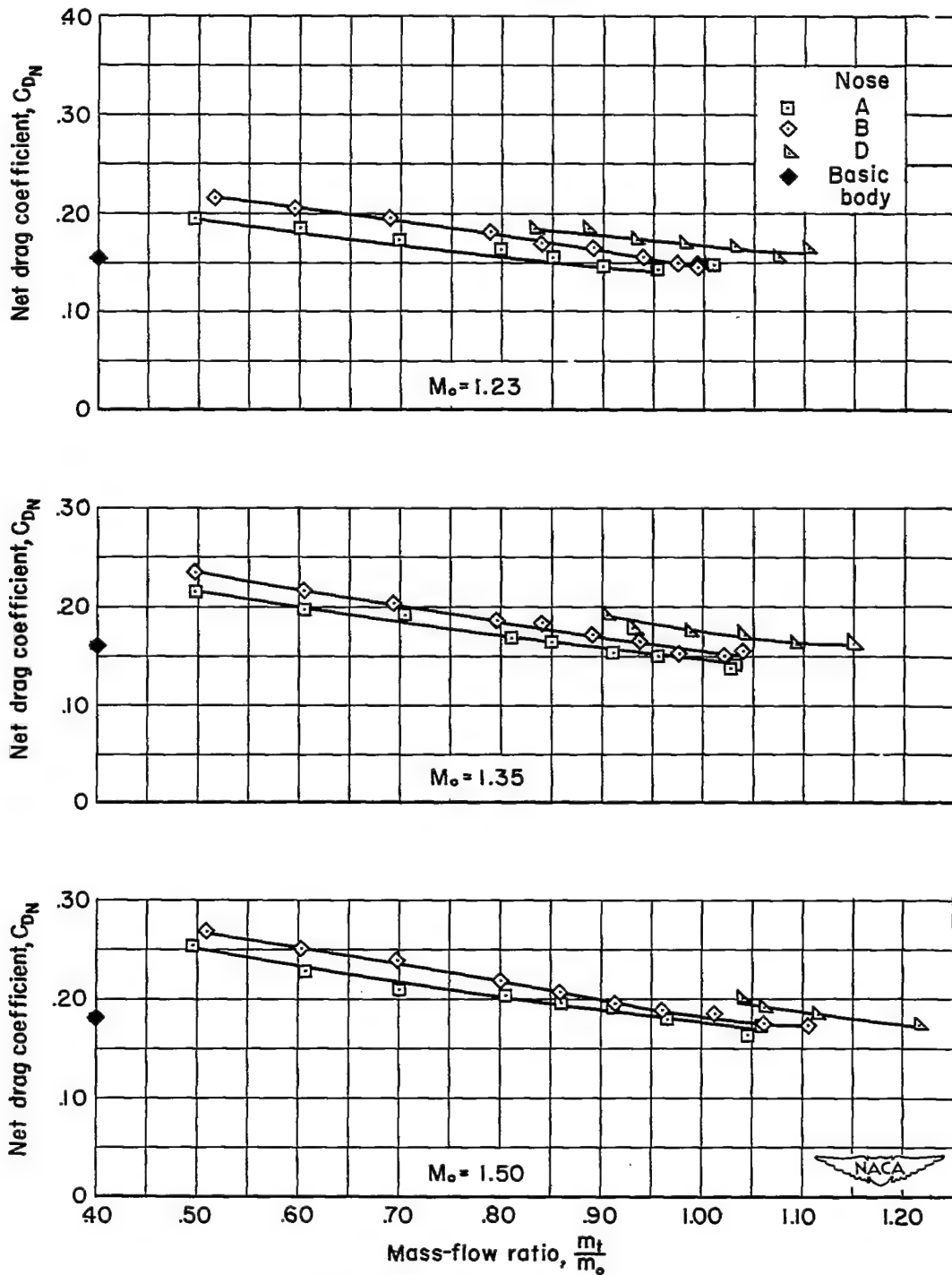
(c) Supersonic Mach numbers, $\alpha = 5^\circ$

Figure 9.- Concluded.

~~CONFIDENTIAL~~

~~CONFIDENTIAL~~

NACA RM A54E06

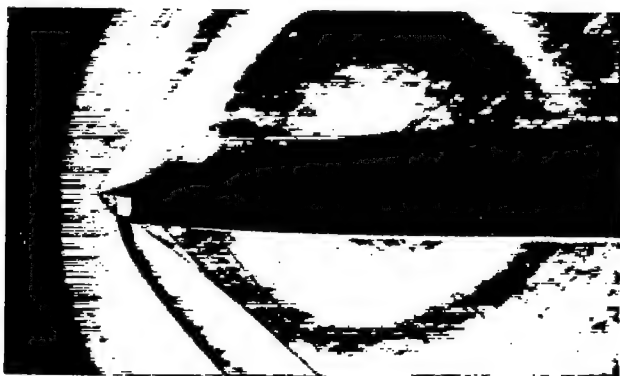
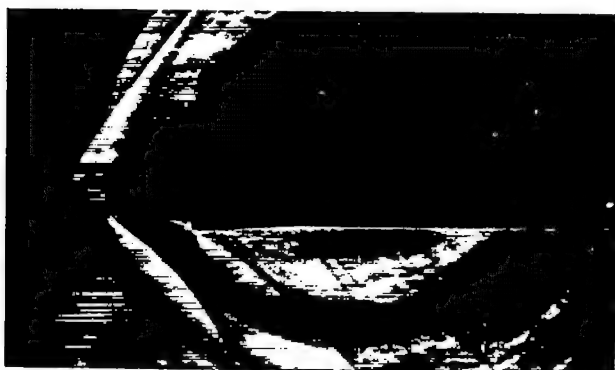
Nose B $M_0 = 1.50$ Nose D $M_0 = 1.35$ Nose D $M_0 = 1.23$

Figure 10.- Schlieren photographs showing flow patterns associated with the flow deflector and auxiliary scoop;

$$\frac{m_t}{m_0} = 0.85, \alpha = 0^\circ.$$

~~CONFIDENTIAL~~

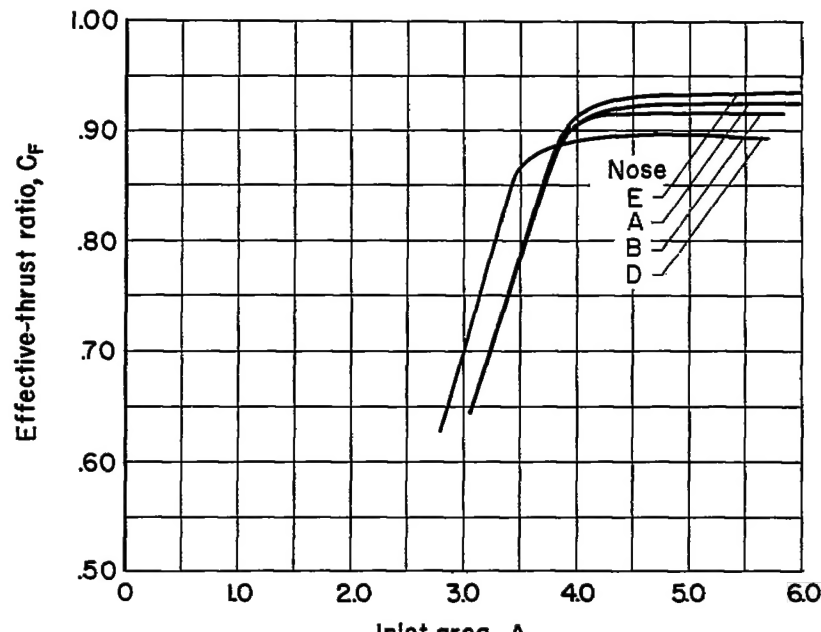
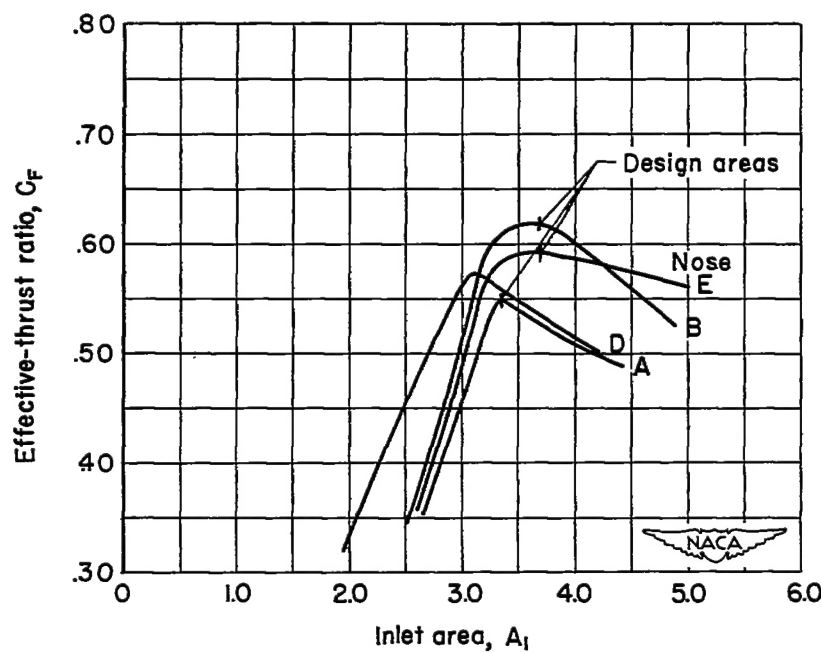
(a) $M_\infty = 0.80$ (b) $M_\infty = 1.50$

Figure 11.- The variation of effective-thrust ratio with duct inlet area for matched inlet-engine operating conditions; 35,000-foot operating altitude; $\alpha = 0^\circ$.

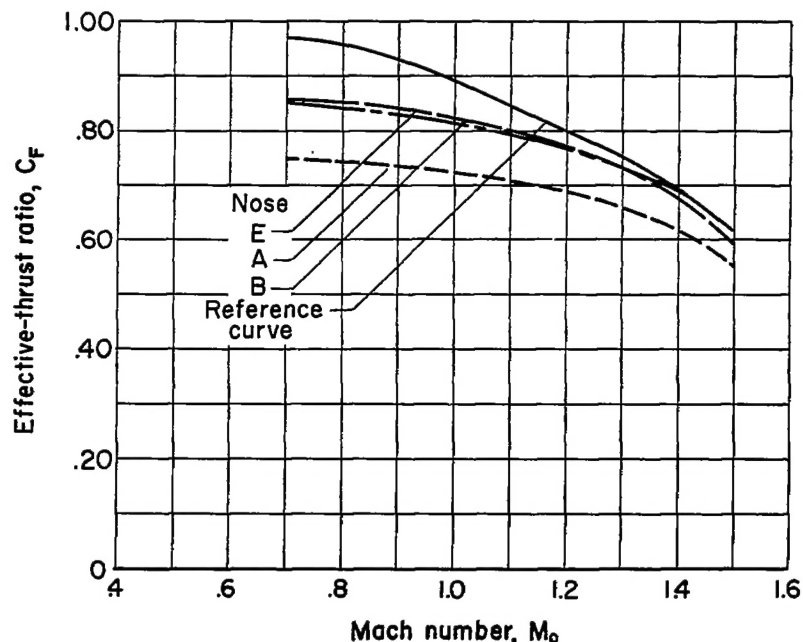
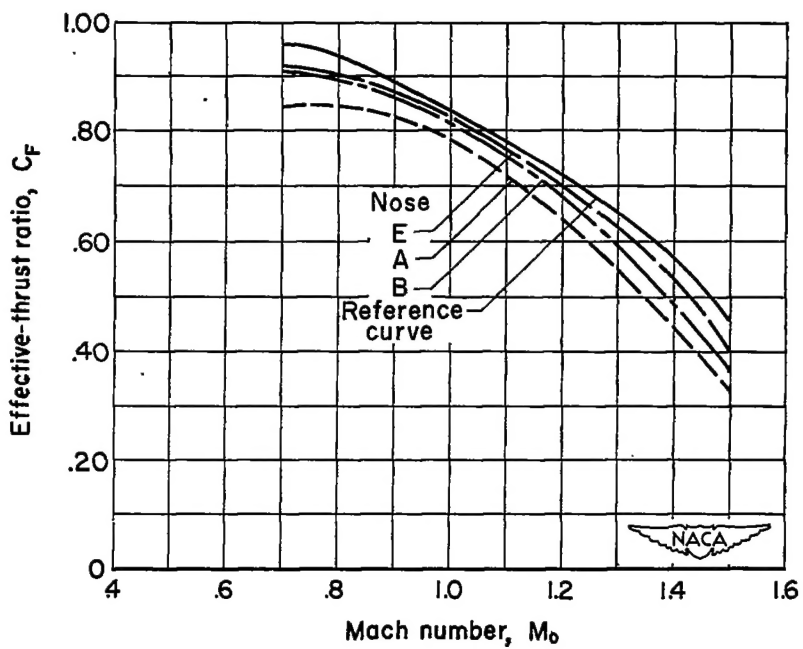
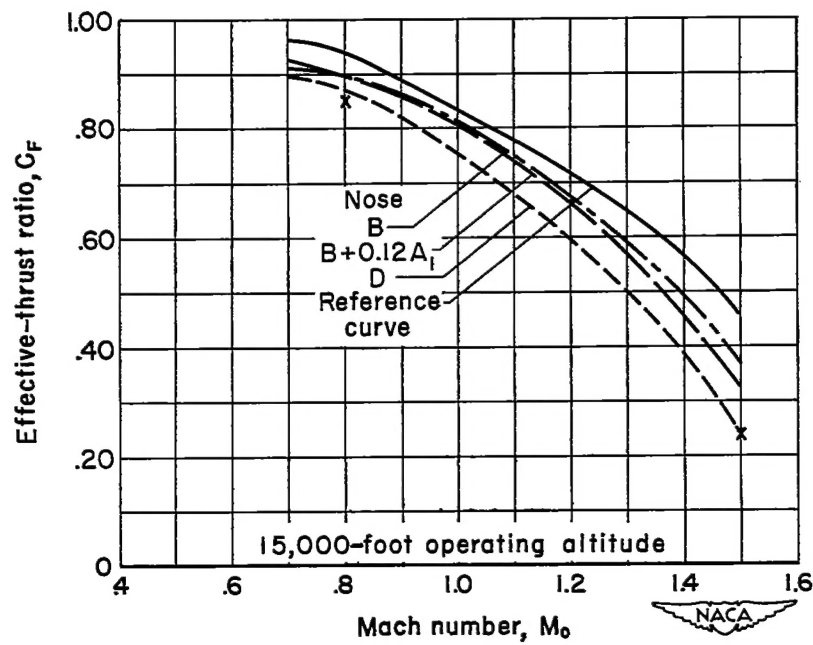
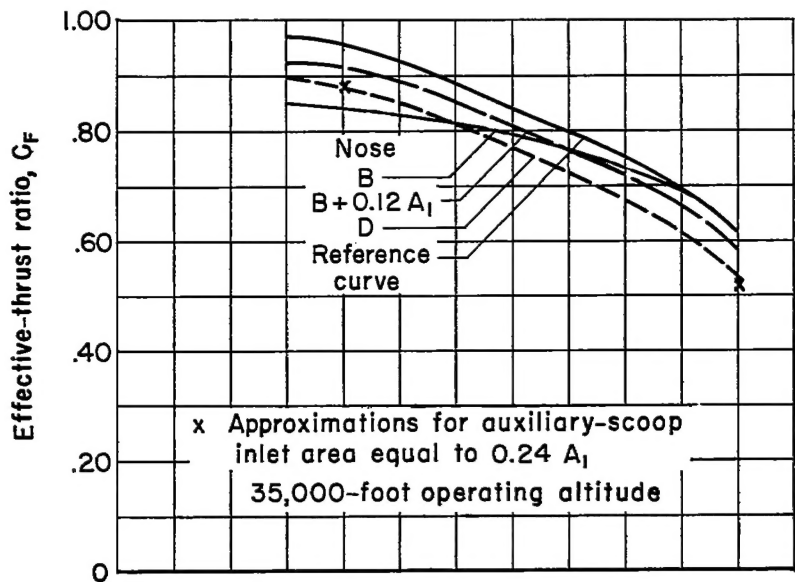
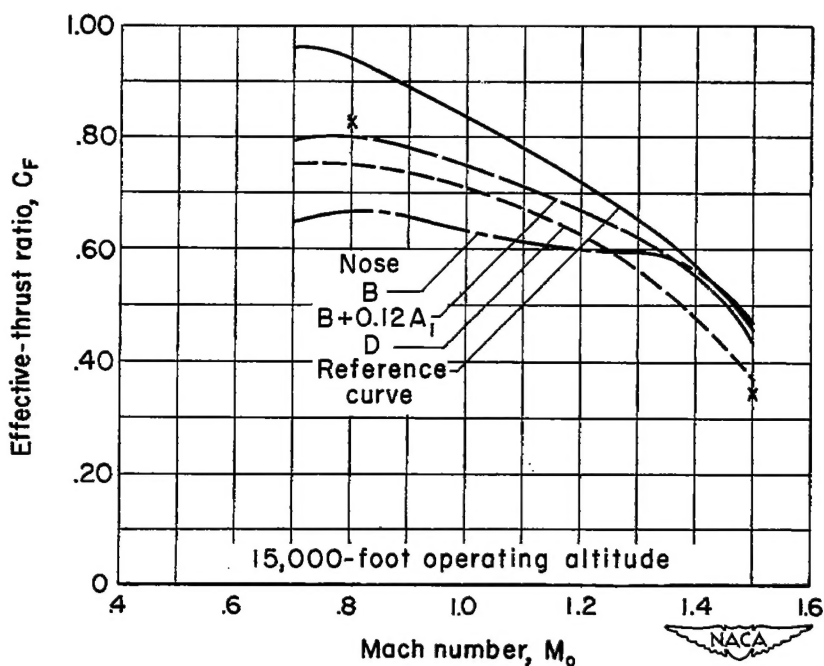
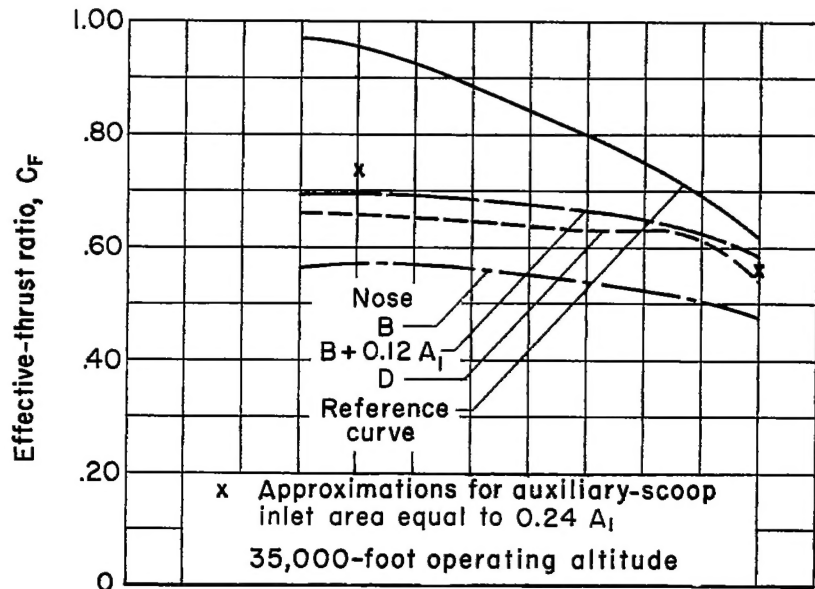
(a) $h = 35,000$ feet(b) $h = 15,000$ feet

Figure 12.- The effect of flow deflectors on the effective thrust ratio of an open-nose inlet; 35,000-foot design altitude; 1.50 design Mach number; $\alpha = 0^\circ$.



(a) 35,000-foot design altitude

Figure 13.- The effect of auxiliary scoops on the effective thrust ratio of an open-nose inlet with a flow deflector; 1.50 design Mach number; $\alpha = 0^\circ$.



(b) 15,000-foot design altitude

Figure 13.- Concluded.